ISSN1027-5495. Functional Materials, 32, No.4 (2025), p. 586-594
doi:http://dx.doi.org/10.15407/fm32.04.586

Features of phase and structure formation in a titanium matrix composites reinforced with a multicomponent alloy of the Ti-Fe-Mn-Si-C(B) system

O. Baranovska[1], A. Bondar[1], G. Bagliuk[1], D. Baranovskiy[1], Ye. Kyryliuk[1], A. Ahapov[2], O. Olifan[1], S. Korichev[1]

[1] Frantsevich Institute for Problems of Materials Science National Academy of Science of Ukraine, Kyiv
[2]Technical Center of the National Academy of Science of Ukraine, Ukraine, Kyiv

Received Aprile 15, 2025

The work is dedicated to the study of phase and structural evolution in titanium matrix composites reinforced with a pre-synthesized master alloy of the TiH_2 – FeSiMn – B_4C system. The composite was fabricated using powder metallurgy techniques, employing PTM-1 grade titanium powder and a pre-synthesized TiH_2 - FeSiMn - B_4C master alloy in varying weight percentages (10, 20, and 30 wt. %) followed by vacuum sintering at 1100 – 1200 °C. The influence of sintering temperature and master alloying element concentration on porosity, microstructure, phase composition, and microhardness was analyzed. The composites sintered at 1200 °C exhibited lower porosity and higher microhardness due to intensified diffusion processes. SEM, XRD, and microprobe analysis confirmed the availability of reinforcing phases such as TiB, $TiC_{0.5}$, and Ti_5Si_3B, and revealed a clear dependence of phase morphology and grain structure on the master alloy content. Microhardness increased with increasing reinforcement content and sintering temperature, reaching peak values of up to 12 GPa in regions enriched with high-modulus compounds in the composite with 30 wt.% master alloy.

Keywords: Titanium matrix composites, powder metallurgy, master alloy, high-modulus reinforcements, microstructure, α-Ti, ß-Ti

Особливості фазо- та структуроутворення титаноматричного композиту армованого багатокомпонентною лігаурою системи Ti-Fe-Mn-Si-C(B).
О. В. Барановська, А. А Бондар, Г. А .Баглюк, Д. І. Барановський, Є.С. Кирилюк, А.І. Агапов, О.І. Оліфан, С.Ф. Корічев

Робота присвячена дослідженню фазо- та структуроутворення титаноматричних композитів, армованих попередньо синтезованою лігатурою системи TiH_2 – FeSiMn – B_4C. Композити виготовляли методами порошкової металургії з використанням титанового порошку марки ПТМ-1 і попередньо синтезованої лігатури системи TiH_2 - FeSiMn - B_4C із різним співвідношенням (10, 20 і 30 мас. %) з подальшим спіканням у вакуумі при 1100–1200 °С. Було проаналізовано вплив температури спікання та концентрації лігатури на пористість, мікроструктуру, фазовий склад та мікротвердість. Показано, що композити, спечені при 1200 °С, мали меншу пористість та більшу мікротвердість внаслідок інтенсифікації дифузійних процесів. За результатами СЕМ, РДА та мікрозондового аналізу підтверджено наявність таких зміцнюючих фаз, як TiB, $TiC_{0,5}$, та Ti_5Si_3B, а також встановлено залежність морфології фаз і зеренної структури від вмісту лігатури. Мікротвердість збільшувалась із підвищенням вмісту армуючих частинок і температури спікання, досягаючи пікових значень до 12 ГПа в областях, насичених високомодульними сполуками, у композиті з 30 мас.% лігатури.

1 Introduction

The search for new materials with high mechanical properties and affordable cost is a relevant task in modern metallurgy. Titanium alloys, due to their unique properties, are promising materials for a wide range of applications. However, traditional titanium alloys often contain expensive rare elements such as V, Mo, Nb, and Ta, which limits their use. To enhance strength and economic efficiency, modern research focuses on strengthening titanium alloys with widely available elements such as silicon, aluminum, iron, and manganese. This approach allows us to increase the tensile strength and ductility of materials without using expensive rare metals [1, 2, 3, 4].

Alloying elements influence the stabilization of the ß-phase and determine both the phase composition and the mechanical properties of the alloys. The study of the structural stability of ß-titanium alloys is often associated with the development of multicomponent systems containing both ß-stabilizers (e.g., Mo, Nb, Ta) and elements with a low Young's modulus (e.g., Sn, Zr, and Al) [5].

According to phase diagrams, elements Fe, Cr, Cu, Ni, Co, and Mn form eutectoid phases with titanium. According to the theory of Bani and Zhou [5], their Mo-equivalent coefficient exceeds 1.0, indicating their significantly greater ability to stabilize the ß-phase compared to monotectoid elements such as Mo, W, and V. For example, Fujii and Maeda [6] noted that titanium alloys with added iron exhibit higher tensile strength than traditional titanium alloys with rare earth elements. Majima [7] demonstrated that the Ti-6Fe wt.% alloy exhibited improved mechanical properties after quenching from the temperature range of single-phase ß.

Manganese in titanium alloys has the same effect as aluminum [8]. The use of Mn as an alloying element in traditional titanium alloys has been considered in binary Ti-8Mn. This alloy was developed for aircraft and structural parts. Like Fe, Mn is a strong eutectoid ß-stabilizer, provides solid solution strengthening, and has a high diffusion coefficient in Ti. The introduction of Mn into titanium alloys significantly increases the hardness of the material up to 122 GPa ($Ti_{12}Mn$), but reduces its ductility [9, 10]. Studies of binary Ti-Mn alloys [11, 12] obtained by powder metallurgy methods have shown that hot deformation after sintering affects the mechanical properties. With a Mn content of 8 to 13 wt.% in the alloys, the formation of a brittle ω-titanium phase is observed [12]. The development of new titanium alloys and the implementation of non-traditional metallurgical methods are relevant for reducing material and production costs. One of the key approaches is the use of inexpensive alloying elements to reduce the cost of titanium alloys. ß-stabilizers such as Fe and Mn are promising for creating new cost-effective alloys. Powder metallurgy is an ideal method for the production of such alloys, since it not only reduces energy consumption but also ensures high initial yield and minimizes the number of production stages [13, 14].

To date, a large number of composite titanium matrix alloys have been created, for the alloying which various reinforcing compounds are used, such as Ti_5Si_3, CrB, B_4C, SiC, TiC, TiN, TiB, and Al_2O_3 [15, 16]. It should be noted that for the reinforcement of titanium, one or several of the above reinforcing compounds are usually used. The most studied composites based on titanium and its alloys, reinforced with SiC and Al_2O_3 fibers or TiC particles, demonstrate high strength, hardness, and wear resistance. In recent years, TiB [17, 18] has been recognized as the most suitable reinforcing material for the titanium system due to its thermodynamic and mechanical stability, as well as the ability to create minimal residual stresses. However, of great interest is the possibility of using a multi-component matrix titanium powder as a strengthening additive, which combines most of the above strengthening particles, such as TiC, TiB, Ti_5Si_3, as well as other promising strengthening phases, such as $Mn_{0.52}Ti_{0.48}$ and Ti_3SiC_2. The use of multiphase composites also opens up new opportunities for optimizing mechanical properties by controlling the microstructure and distribution of strengthening phases in the matrix.

In previous works [19, 20], we investigated the influence of ferroalloys containing titanium ß-stabilizers, such as Fe, Mn, Si, on the structure and phase composition of titanium alloys. Boron carbide compound B_4C was used as a source of carbon and boron. As a result of thermal synthesis, we obtained a compact containing the following phases: TiC, Ti_5Si_3, TiB, $Mn_{0.52}Ti_{0.48}$, and Ti_3SiC_2. During sintering, boron carbide and titanium powders interact to form thermodynamically stable TiB particles uniformly distributed throughout the titanium alloy matrix with clear interphase boundaries, as well as titanium carbide (TiC) particles, which are important for further increasing the

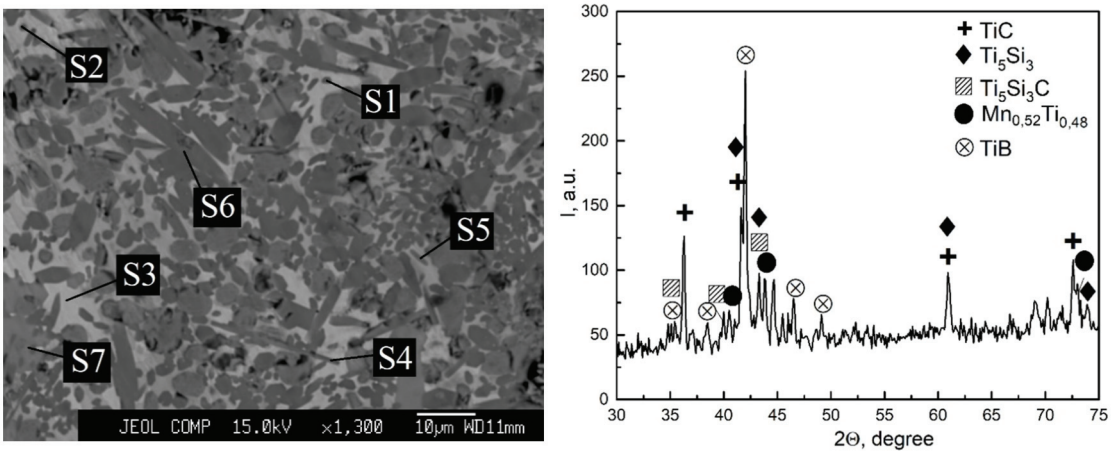

Fig. 1 SEM images of the thermally synthesized multicomponent composite structure (a) (phase components: S1, S2 – TiC; S3 – Ti–Mn system; S4, S5 – TiB; S6, S7 – Ti–Si system) and fragment of the diffraction pattern of a master alloy of the TiH_2 – FeSiMn – B_4C system synthesized at 1250 °C (b)

hardness and wear resistance of the material. A small addition of boron (B) or borides (B_4C) significantly improves the microstructure of sintered titanium alloys and also affects the change in the morphology of α-Ti [21, 22, 23, 24]. In [21], for the first time in the process of powder metallurgy (PM) of titanium alloys, a small amount of boron and boride powders (B_4C and B_4Si) was first used, which led to a significant refinement of previously formed ß-grains.

Thus, **the aim of this work** is to study the phase and structural components of titanium matrix composites reinforced with multicomponent strengthening particles TiC, Ti_5Si_3, TiB, etc. The use of such strengthening materials opens up prospects for creating cost-effective and high-performance composites that can compete with traditional titanium alloys. This will reduce production costs and improve the mechanical properties of titanium matrix composite materials.

2 Experimental materials and methods

For the fabrication of the powder metallurgy titanium matrix composite, titanium powder of PTM-1 grade (0.08 N; 0.05 C; 0.35 H; 0.40 Fe+Ni; 0.1 Si; 0.004 Cl) according to TU 14-22-57-92 and a pre-synthesized, milled master alloy of the TiH_2 – FeSiMn - B_4C system were used (details regarding the master alloy production technology and its properties are described in previous studies [19, 20]). The microstructure of the synthesized composite material and a fragment of its diffraction pattern are depicted in Figure 1.

The composite powder mixture was prepared in the following ratios:

1. 90 Ti + 10 wt. % master alloy;
2. 80 Ti + 20 wt.% master alloy;
3. 70 Ti + 30 wt.% master alloy.

The mixed powders were compacted at 650 MPa. The pressed compacts were sintered in an SShVL-1.2.5/25-M04 vacuum furnace at temperatures ranging from 1100 to 1200 °C for 1 hour. The density and porosity of the obtained composites were determined according to DSTU ISO 2738:2009. The microstructure of the composites was studied using a JEOL scanning electron microscope (JEOL Ltd, Japan, 2007), and a JXA-8200 electron probe microanalyzer, which allows measuring the chemical composition of materials. The phase composition of the samples was determined by X-ray diffraction in filtered Co-K_α radiation (λ = 0.15418 nm) using a DRON-3M diffractometer at 20–130° with step-by-step scanning. Vickers microhardness tests were performed on a PMT-3 device under a load of 0.5 kg for 30 s, and the average value of seven measurements was taken for each sample.

3 Results and discussion

The results of the experimental sintering (Figure 2) at 1100°C show that for all samples, the initial sintering stage is characterized by minimal shrinkage and lower density of the material. Samples sintered at 1200°C demonstrate a significantly denser structure. The increase in temperature led to better compaction of the material, resulting in a more homogeneous surface, especially in the case of higher concentra-

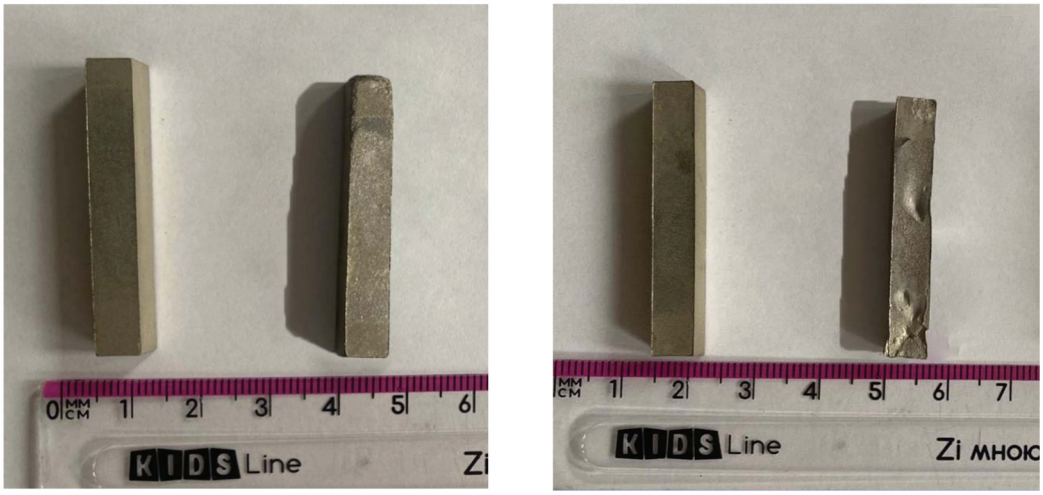

a b

c

Fig. 2 External appearance of the Ti + 10 wt.% master alloy (a), Ti + 20 wt.% master alloy (b), and Ti + 30 wt.% master alloy (c) samples after sintering at temperatures of 1100 °C (left) and 1200 °C (right).

tions of alloying phases. Figure 2 shows the appearance of titanium-based alloy samples with varying master alloy concentrations (10 %, 20 %, 30 % (wt.)) after sintering at two different temperatures: 1100°C and 1200°C.

Figure 3 illustrates the dependence of the porosity of the composite materials on the sintering temperature and master alloy content. According to these data, increasing the sintering temperature from 1100 °C to 1200 °C for all the compositions studied leads to a decrease in porosity.

The composites containing 10 wt.% of reinforcing particles exhibit the highest porosity at both 1100 °C and 1200 °C. However, with an increase in the master alloy content to 20 wt.% and 30 wt.%, the porosity decreases, especially at the higher sintering temperature. Increasing the fraction of reinforcing components to 20 wt.% reduces the composite porosity by approximately 1.35–1.5 times compared to composites containing 10 wt.% of reinforcing particles. The samples with 30 wt.% master alloy have the lowest porosity, which reaches 9 % at a sintering temperature of 1200 °C, which is 2.2 and 3 times lower compared to the composite containing 20 and 10 wt.% of reinforcing particles, respectively. It should be noted that with an increase in the sintering temperature, a tendency towards a decrease in the porosity of samples of all compositions is observed. This is explained by the intensification of diffusion processes and the activation of mass transfer mechanisms at elevated temperatures, which leads to a reduction in pore size and their coalescence. The increase in the amount of liquid phase in the alloys when the temperature rises to 1200 °C promotes the movement of titanium particles and their convergence with each other. This leads to an increase in the contact area between the particles and promotes their denser packing. Within this temperature range, diffusion pro-

Table 1. Element content (at.%) at different points of the sintered composites

Spectrum No	Ti	Mn	Fe	Si	B	C	Structural Components
1	94.75	0.61	2.82	0.23	—	1.60	(ß-Ti)*
2	97.72	0.01	0.00	0.24	—	2.03	(α-Ti)*
3	71.97	0.02	0.02	0.02	19.87	8.10	HMR
4	93.67	0.67	3.72	0.24	—	1.70	(ß-Ti)
5	97.80	0.06	0.06	0.29	—	1.79	(α-Ti)
6	52.05	0.00	0.12	0.11	43.57	4.15	HMR
7	91.87	1.37	4.94	0.89	—	0.93	(ß-Ti)
8	97.27	0.10	0.03	0.62	—	1.98	(α-Ti)
9	52.40	0.04	0.04	0.32	42.58	4.62	HMR

Note: ()* indicates a solid solution based on α- or ß-Ti

cesses are localized near the grain boundaries of titanium. Free protrusions and defective areas of the grains dissolve, and coagulated atoms are deposited in more equilibrium areas, which helps bring the grains closer to their equilibrium shape. The X-ray diffraction patterns of the samples after sintering at temperatures of 1100 and 1200 °C are shown in Figure 4.

The X-ray diffraction analysis shows that all the samples are predominantly composed of hexagonal α-Ti. For composites containing 10 and 20 wt.% of the master alloy, the peak corresponding to the α-Ti (101) plane consistently exhibits the highest relative intensity. When introducing 10 wt.% of the master alloy and a sintering temperature of 1100 °C, peaks of titanium carbide TiC are present. Upon increasing the sintering temperature to 1200 °C, peaks of rhombic TiB appear on the diffraction pattern, which are recorded at 2θ angles of 38 and 52°. With an increase in the reinforcing particle content to 20 wt.%, along with TiC and TiB, the formation of a small amount of the ternary phase Ti_5Si_3B is observed. The content of 30 wt.% reinforcing particles leads to an increase in the number and intensity of TiC and Ti_5Si_3B peaks.

The results of micro X-ray structural analysis fully correlate with the X-ray diffraction patterns described above. Quantitative analysis (Figure 5, Table 1) showed that the light gray areas in the microstructure photographs consist mainly of 91–94 at.% titanium, as well as some Mn, Fe and Si, and may represent a solid solution based on ß-Ti (Table 1, spectra 1, 4, 7). The gray areas correspond to a solid solution

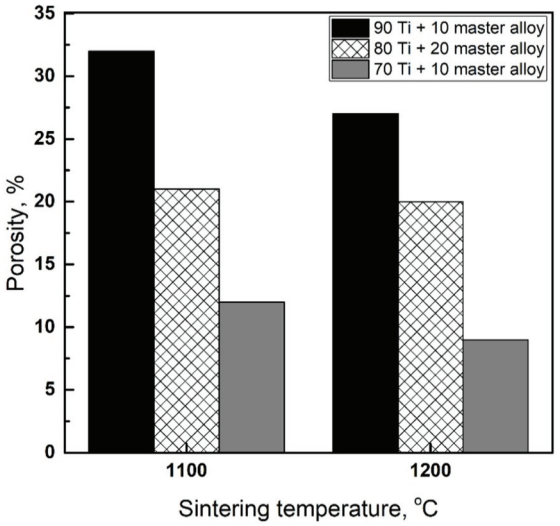

Fig. 3 The influence of sintering temperature on the porosity of the composites

based on α-titanium, with a titanium content of approximately 98 at.% (Table 1, spectra 2, 5, 8). The dark gray areas consist of high-modulus reinforcements (HMR) of the TiB, $TiC_{0.5}$, and Ti_5Si_3B types (Table 1, spectra 3, 6, 9).

A detailed quantitative analysis of the microstructure of the sintered composites showed that the addition of the alloying component significantly affects the grain size and the morphology of the α-Ti-based phase (Fig. 5). Although visual identification of the ß-Ti-type phase in the microstructural images is difficult due to its small quantity, the X-ray diffraction data clearly confirm the presence of this phase. It is known that iron and manganese atoms have a wide homogeneity range in titanium, which leads to their partial dissolution in the

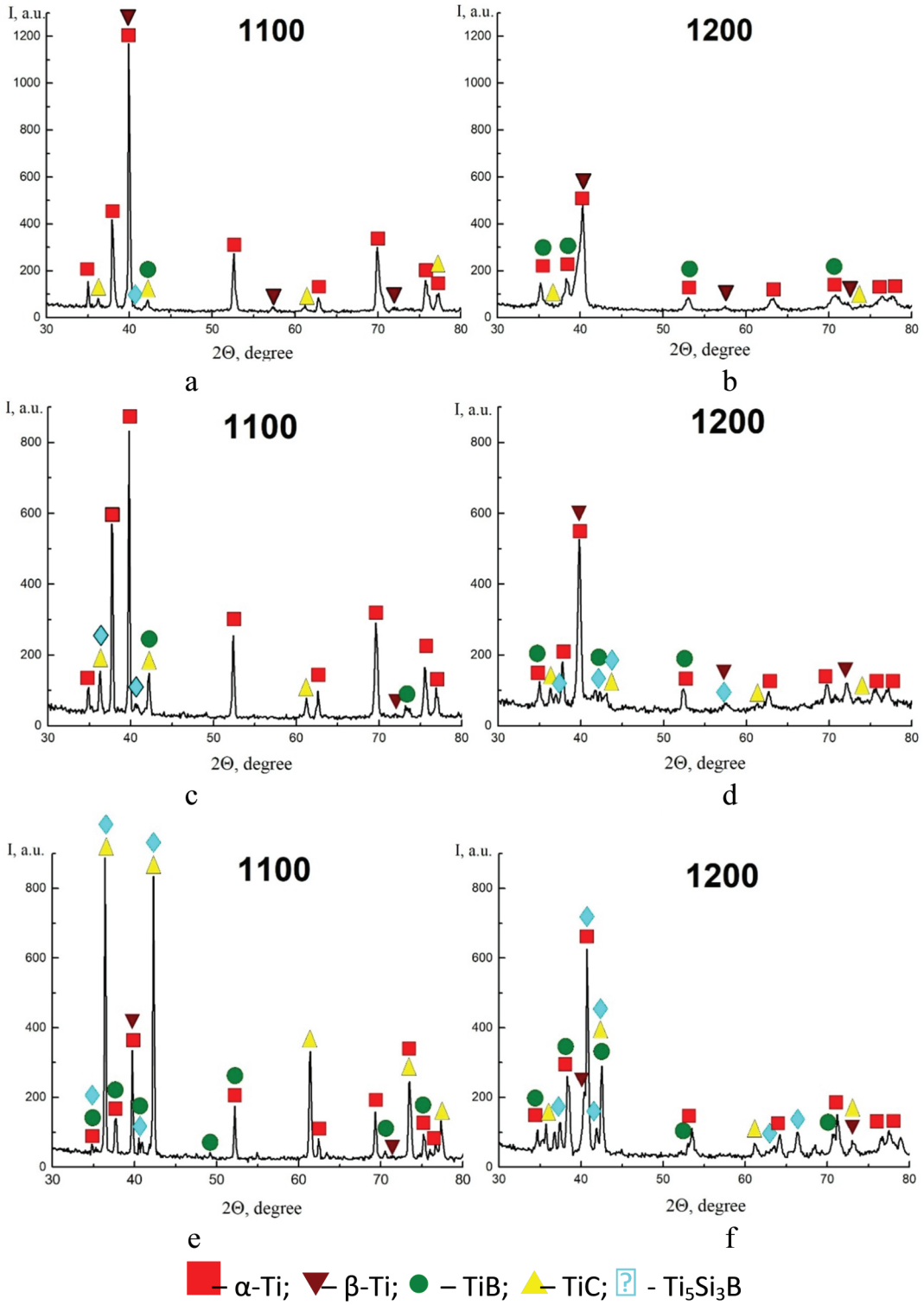

Fig. 4 Fragments of the X-ray diffraction patterns of composites containing 10 wt.% (a, b), 20 wt.% (c, d), and 30 wt.% (e, f) master alloy after sintering at 1100 °C and 1200 °C

Ti matrix. According to [25], ß-phase be formed the regions of Fe and Mn dissolution. Moreover, the authors noted that Fe atoms significantly contribute to the refinement of α-phase grains. This indicates the effectiveness of adding stabilizers (Fe and Mn) to ß-Ti, which, according to the molybdenum equivalent (MoE) definition

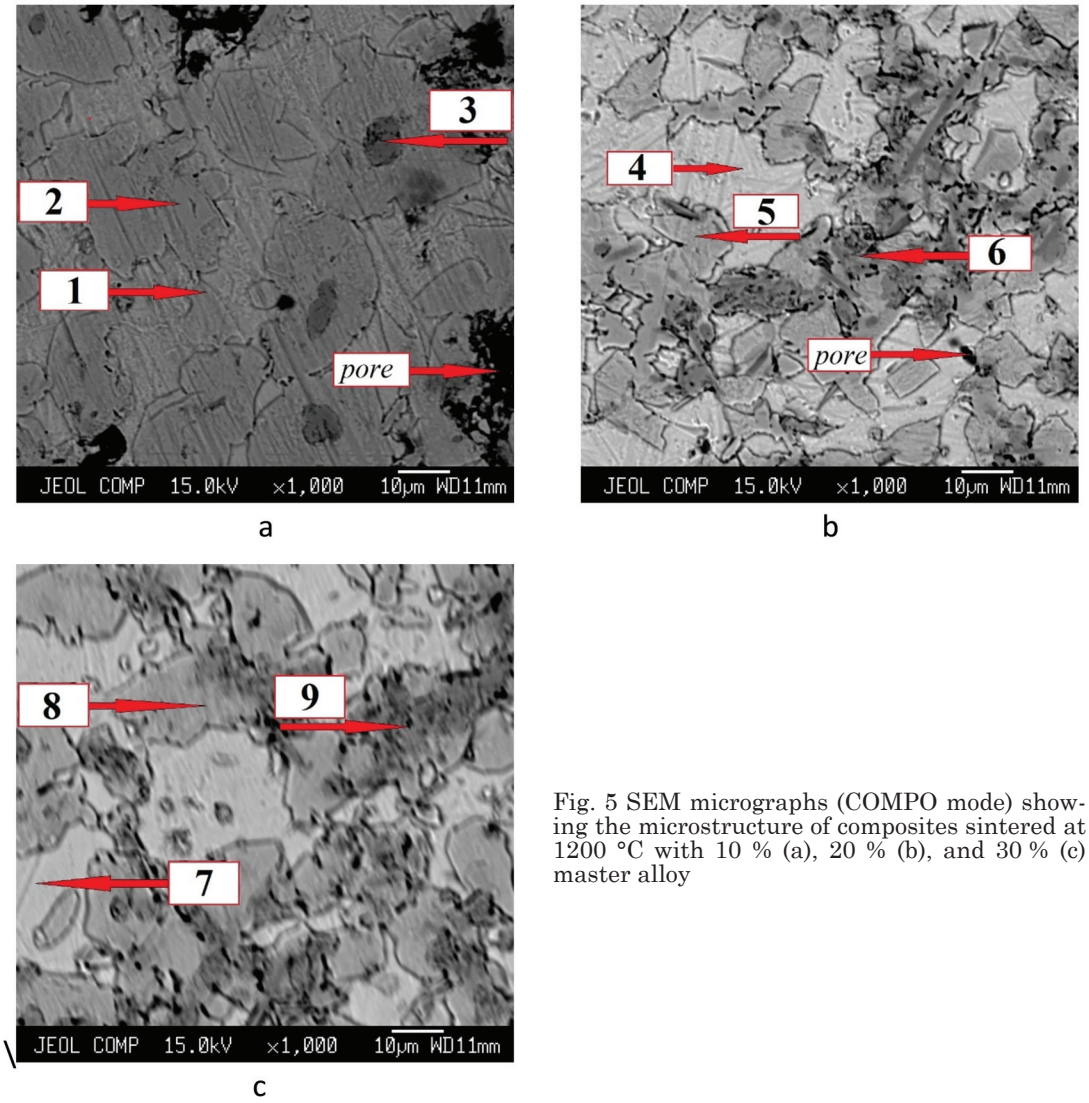

Fig. 5 SEM micrographs (COMPO mode) showing the microstructure of composites sintered at 1200 °C with 10 % (a), 20 % (b), and 30 % (c) master alloy

[26], promote the formation and stabilization of the ß-phase even in small amounts.

Depending on the alloying content and sintering temperature, strengthening particles of the TiB, $TiC_{0.5}$, and Ti_5Si_3B types are observed inside the α-Ti-based phase and, to some extent, outside the α-Ti phase. The authors of [27] state that at 882 °C during cooling, a peritectoid reaction occurs (according to the Ti-B phase diagram: ß-Ti + TiB → α-Ti), which coincides with the α→ß transformation (at 881 °C). According to this reaction, TiB can act as a nucleation site for the α-Ti phase if their lattice parameters are well-matched. Based on the X-ray diffraction results, the lattice parameters of TiB (orthorhombic) are a = 6.020 Å, b = 3.038 Å, and c = 4.256 Å. These b and c parameters correspond to a and c parameters of the α-Ti phase (hexagonal, a = 2.940 Å, c = 4.68 Å), respectively. TiB particles formed during heating above 700 °C or precipitated from the ß-Ti phase during cooling may serve as nucleation sites for the α-Ti phase. This also explains why most TiB particles are located inside the α-Ti grains. Furthermore, the authors of [27] note that the boron contained in titanium alloys leads to the formation of nearly equiaxed α-Ti grains and also restricts the growth of ß-phase grains.

The sintering temperature and the increased content of reinforcing particles lead to an increase in microhardness compared to the unreinforced titanium alloy. To assess the influence of the reinforcing particles on microhardness, an area free from pores and containing various microstructural components typical of the investigated material was selected. The composite matrix, which mainly consists of titanium and small amounts of Mn and Fe, exhibits

Table 2. Effect of alloying additive content and sintering temperature on the microhardness of titanium matrix composites

Master alloy content, wt.%	Sintering temperature, °C	Structural component	Microhardness (HV), GPa
90 Ti + 10 master alloy	1100	(β -Ti) (α -Ti) HMR	3.38÷4.32 5.45÷5.93 —
	1200	(β -Ti) (α -Ti) HMR	3.32÷3.48 6.01÷6.5 —
80 Ti + 20 master alloy	1100	(β -Ti) (α -Ti) HMR	4.15÷4.72 5.71÷6.16 8.06 ÷ 9.42
	1200	(β -Ti) (α -Ti HMR	4.6÷5.8 6.1÷7.5 8.25÷10.87
70 Ti + 30 master alloy	1100	(β -Ti) (α -Ti) HMR	4.8÷5.9 7.86÷8.85 9.56÷11.35
	1200	(β -Ti) (α -Ti) HMR	4.63÷5.62 7.36÷9.47 10.86÷12.01

the lowest hardness, ranging from 3.48 to 5.9 GPa, depending on the content of reinforcing particles and the sintering temperature. The α-Ti grains containing some carbides or borides demonstrate slightly higher hardness, in the range of 6.01 to 9.4 GPa. The highest hardness values were measured for phases identified as Ti combined with high-modulus reinforcements, reaching 8.06 to 12.1 GPa, depending on the content of reinforcing particles (Table 2).

It should be noted that titanium boride compounds exhibit higher hardness compared to other high-modulus compounds distributed within the titanium grains. Therefore, the heterogeneity of hardness within individual grains may be associated with the uneven clustering of reinforcing particles. These clusters may lead to localized increases in hardness in specific regions of the grains.

The hardness of titanium alloys depends largely on their microstructure, which in turn is determined by processing and heat treatment. According to previous studies, depending on the processing method, thermal treatment, or phase composition, materials with the same chemical composition may demonstrate significantly different hardness values [28, 29].

The obtained microhardness values are consistent with the literature data. For example, ß-titanium alloys quenched from the ß-phase region typically exhibit hardness in the range of 2.74–3.04 GPa, while an increased fraction of the α-phase results in a hardness range of 4.51–4.9 GPa [30]. Additionally, the authors of [31] obtained similar hardness values for the matrix and demonstrated that the hardness of the reaction layer identified as a mixture of TiB and TiC reached 13.3 GPa (Table 2), which also corresponds to the microhardness of the composite with 30 wt.% additive in the region of clustered high-modulus compounds.

Conclusions

The results of this study allow us to draw the following conclusions:

1. A significant dependence of the structure and phase composition of the composite alloys on the alloying additive content and sintering temperature has been demonstrated. Samples with a higher concentration of the additive (20% and 30%) show a lower level of porosity compared to those containing 10%, especially when sintered at 1200 °C. This is attributed to enhanced diffusion processes and the activation of mass transfer mechanisms that promote material densification.

2. X-ray diffraction analysis revealed that all sintered samples consist predominantly of hexagonal α-Ti, with a dominant (101) diffraction peak. The detection of a small amount of ß-Ti phase confirms its stabilization under cer-

tain chemical composition conditions. In the composite with 10 wt.% additive and a sintering temperature of 1200 °C, peaks of titanium carbide (TiC) and titanium boride (TiB) were observed. Increasing the content of reinforcing particles to 20 wt.% resulted in the formation of the ternary phase Ti_5Si_3B along with TiC and TiB.

3. Micro-X-ray spectral analysis identified the presence of three structural zones: a composite matrix (Ti + Fe, Mn, Si), α-Ti grains, and high-modulus reinforcement particles, such as TiB, $TiC_{0.5}$, and Ti_5Si_3B. Furthermore, the study demonstrated that both the amount of alloying additive and the sintering temperature played a significant role in determining the morphology and grain size of the α-Ti phase.

4. The microhardness of the sintered composite was shown to be influenced by both the sintering temperature and the reinforcing particle content. The composite with the lowest reinforcing particle content (10 wt.%) exhibited the lowest hardness. A positive correlation was observed between increasing sintering temperature and reinforcing particle content, and the resulting microhardness of the structural components. Notably, in the Ti + 30 wt.% composite, the matrix hardness ranged from 4.63 and 5.62 GPa, the α-Ti phase microhardness ranged from 7.36 and 9.47 GPa, and the zone with the highest concentration of high-modulus reinforcements displayed the highest microhardness values – from 10.86 to 12.01 GPa.

References

1. T. Mimoto, J. Umeda, K. Kondoh. *Powder Metall.*, **59**, 223 (2016).
2. Y. Yamabe, J. Umeda, H. Imai et al. *Mater. Trans.*, **59**, 61 (2018).
3. S. Kariya, M. Fukuo, J. Umeda, K. Kondoh et al. *Materials*, **14(21)**, 6561 (2021).
4. B. Chen, J. Shen, X. Ye et al. *J. Mater. Res.*, **32**, 3769 (2017).
5. Q. Wang, C. Dong, P.K. Liaw. *Metall Mater Trans A* **46**, 3440 (2015).
6. H. Fujii, T. Maeda. *Nippon Steel Tech. Rep.*, **106**, 16 (2014).
7. K. Majima, T. Isono, K. Shoji. *J. Jpn. Soc. Powder Metall.*, **34**, 349 (1987).
8. N. Saunders. *Gamma Titanium Aluminides*, **183** (1999).
9. F. Zhang, E. Burkel. *J. Biomed. Eng., **9**, 203* (2011).
10. H.J. Breme, V. Biehl, J.A. Helsen. *Biomaterials Science and Engineering Series*, Wiley, New York (1998).
11. Y. Alshammari, M. Jia, F. Yang et al. *Mater. Sci. Eng. A*, **769**, 138496 (2020).
12. P. F., Santos, M. Niinomi, H. Liu et al. *J. Mech. Behav,*. **59**, 497 (2016).
13. R.M. German. *IJRMHM,* **89**, 105214 (2020).
14. L. Bolzoni I. M., Meléndez, E. M. Ruiz-Navas et al. *Mater. Sci. Eng.,* **546,** 189 (2012).
15. K. Morsi, & V. V. Patel. *J. Mater. Sci.,* **42,** 2037 (2007).
16. E.R. Gaisina, R.A. Gaisin, V.M. Imayev et al. *Phys. Met. Metallogr.,* **114,** 623 (2013).
17. Ye.G Byba, & P. I. Loboda. *Scientific Bulletin Kherson State Maritime Academy, 2(11),* 137 (2014).
18. K.S.R. Chandran, K.B. Panda, S.S. Sahay, *J. Miner. Met. Mater. Soc.*, **56**, 42 (2004).
19. O. Suprun, G. Bagliuk, O. Shirokov. *Nauk. Notatki,* **66**, 344, (2019) [in Ukrainian].
20. O.V. Baranovska, O.I. Bykov, G.A. Bagliuk et al. *Mater. Sci.,***57(2)**, 201 (2021).
21. U.S. Patent, **4,601,874** (1986).
22. T. Saito, *Adv. Perform. Mater.*, **2**, 121 (1995).
23. O.M. Ferri, T. Ebel, R. Bormann, *Adv. Eng. Mater.*, **13**, 436 (2011).
24. S.D. Luo, Y.F. Yang, G.B. Schaffer et al. *J. Alloys Comp.*, **555**, 339 (2013).
25. J. Umeda, T. Tanaka, T. Teramae. *Mater. Sci. Eng. A.* 803, 140708 (2021).
26. Q. Wang, C. Dong, P. Liaw. *Metall. Mater. Trans. A.* **46**(8), 3440 (2015).
27. Y.F. Yang, M. Yan, S.D. Luo et al. *J. Alloys Compd.* **579**, 553 (2013).
28. L.C. Campanelli, P.S.C.P. da Silva, C. Bolfarini. *Mater. Sci. Eng. A.* **658**, 203 (2016).
29. K. Zyguła, M. Wojtaszek. *Arch. Metall. Mater.* **65**, 287 (2020).
30. J. Coakley, V.A. Vorontsov, N.G. Jones et al. *J. Alloys Compd.* **646**, 946 (2015)
31. S. Grützner, L. Krüger, C. Schimpf et al. *Metall. Mater. Trans. A.* **49**, 5671 (2018).